

Corrosion Behavior Study of Cr₂₀Mn₁₅Fe₂₀Co₂₅Ni₂₀ High-entropy Alloy in 3.5 Wt.% NaCl Solution

Naresh Kaushik*, Anoj Meena, Vinayak Goswami and Harlal Singh Mali

Advanced Manufacturing and Mechatronics Lab, Department of Mechanical Engineering, Malaviya National Institute of Technology Jaipur, Jaipur, Rajasthan, India

*Correspondence to:

Naresh Kaushik

Advanced Manufacturing and Mechatronics Lab,
Department of Mechanical Engineering,
Malaviya National Institute of Technology Jaipur,
Jaipur, Rajasthan, India.

E-mail: 2019rme9084@mmit.ac.in

Received: November 24, 2022

Accepted: April 28, 2023

Published: April 30, 2023

Citation: Kaushik N, Meena A, Goswami V, Mali HS. 2023. Corrosion Behavior Study of Cr₂₀Mn₁₅Fe₂₀Co₂₅Ni₂₀ High-entropy Alloy in 3.5 Wt.% NaCl Solution. *NanoWorld J* 9(S1): S491-S494.

Copyright: © 2023 Kaushik et al. This is an Open Access article distributed under the terms of the Creative Commons Attribution 4.0 International License (CCBY) (<http://creativecommons.org/licenses/by/4.0/>) which permits commercial use, including reproduction, adaptation, and distribution of the article provided the original author and source are credited.

Published by United Scientific Group

Abstract

Corrosion behaviour of Cr₂₀Mn₁₅Fe₂₀Co₂₅Ni₂₀ high-entropy alloy is studied with immersion test and electrochemical test in 3.5 wt.% NaCl solution in open environment to test the life of the alloy. In immersion testing, the weight loss percentage obtained for sample for five days and 14 days is 1.02% and 1.44%, respectively. The average surface roughness for sample in immersion testing is 1.879 µm at five days and 1.889 µm at 14 days duration. Corrosion rate obtained using weight loss method is 0.32 mm/year as compared to 0.47 mm/year and 0.30 mm/year for 304L SS and Cu alloy, respectively. Tafel plot shows the corrosion potential E_{corr} value of -319 mV and the I_{corr} value of -5.099 A/cm², and highest open circuit potential (OCP) of -344 mV at 600 seconds, results that sample has increased corrosion resistance capabilities than 304L SS, 201L SS.

Keywords

Cantor alloy, NaCl solution, Pitting corrosion, Open circuit potential, Tafel plot

Introduction

Corrosion plays detrimental effect on the life of the components [1]. Dr. Yeh hypothesized in 1995 that multi-component alloys would've had significant configurational entropy, reduced Gibbs free energy, and encouraged the formation of a simple solid solution or possibly a sophisticated structure, in opposition to the primary mode of thinking [2]. High-entropy alloys (HEAs) are the name given to these alloys. HEAs have raised interest since their launch in 2004 because of their superior mechanical, operational, and corrosion characteristics [3]. These have contributed to answers to critical material difficulties in various industries [4]. HEAs, often called multi-principal element alloys are alloyed with five or more elements with varying concentrations from 5% to 35% [5]. Corrosion behaviour of these has been extensively studied in a variable mode of setting [6]. Elemental alloying changes the corrosion resistance of materials in general. Different elemental alloying can alter corrosion resistance by adjusting phase structure and elemental segregation, affecting the passive layer characteristic, changing the nobility of a phases, and affecting dissolution kinetics [7].

The potentiodynamic-polarization test, a classic electrochemical method, is commonly used to study the corrosion behaviour of a material. Han et al. [8] investigated the corrosion behaviour of CoNiFeCrMn HEA with ultra-fine grains. When compared to a coarse-grained sample, a potentiodynamic test and electrochemical impedance spectroscopy (EIS) revealed that an unstable passive layer formed more quickly on the surface of the UFG Cantor alloy, causing it to show an enhanced corrosion rate.

Nishimoto et al. [9] studied that plasmanitrided CoCrFeMnNi HEAs have microstructural, mechanical, and corrosion characteristics. For nitride materials,

the pitting potential was determined using a 3.5 wt.% NaCl (sodium chloride) aqueous solution. Wang et al. [10] investigated that in a 0.5 M H_2SO_4 environment, the effect of grain size on the rate of corrosion of CoCrFeMnNi HEAs. Increasing it can improve corrosion resistance when the grain size is below a threshold limit. Fine-grained (1.24 μm) HEA develops several grain boundaries, which accelerates galvanic corrosion at grain boundaries with inter-grains as well as reduces corrosion resistance. Moon et al. [11] studied the corrosion of Additively Manufactured CoCrFeMnNi HEAs in molten $\text{NaNO}_3\text{-KNO}_3$. During potentiodynamic polarization testing, the CoCrFeMnNi HEA had such a larger passive current density than steel alloys SS316L and 4130, as well as the high-Ni alloy 800 H. Cr and Ni were discovered to be fully depleted at the oxide's outer surface and dissolved in large amounts in the molten salt.

Materials

Non-equiatomically $\text{Cr}_{20}\text{Mn}_{15}\text{Fe}_{20}\text{Co}_{25}\text{Ni}_{20}$ HEA synthesized using induction melting process is used for the corrosion behaviour study. Samples exposed to an area of 400 mm^2 is used for electrochemical experiments. Before the experiments to be performed sample working surface was abraded using automatic grinder and polishing machine using grit papers 120, 400, 800, 1500, and 2000 sizes according to the standards GB5776-86 followed by polishing on a felt pad having 3 μm and 1 μm diamond paste to get mirror like surface. After all this use ethanol clean the sample surface using cotton wool gently [12]. For the corrosion test, pure crystal of sodium chloride with 99.5% purity, density of 1.023 g ml^{-1} and molecular weight of 58.44 g ml^{-1} by the company name of CDH chemicals is used.

ASTM G44 [13] standard used for immersion corrosion test for metal alloys in a 3.5% NaCl solution. It is used mainly for aluminum and ferrous alloys but can be used for any metal that shows susceptibility to Cl^- ions. It is also used in other solutions, such as synthetic sweat or seawater. For the experimental work, 0.6 M or 3.5 wt.% NaCl is taken as shown in figure 1.

For 100 ml of 0.6 M NaCl chemical solution it needs 3.5 g of NaCl with 96.5 ml of distilled water. As per the standard of ASTM-G31-12a, the immersion test has been performed for the period of 5 days and 14 days duration and determined

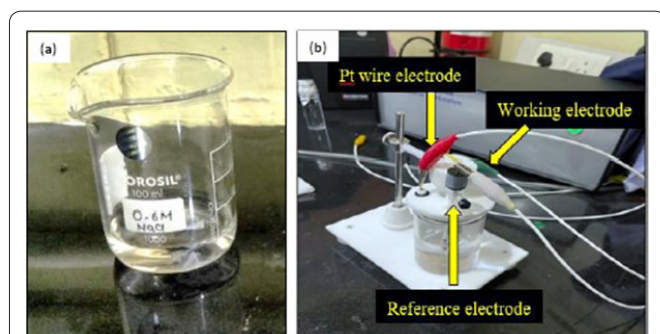


Figure 1: (a) Immersion test setup for non-equiatomically $\text{Cr}_{20}\text{Mn}_{15}\text{Fe}_{20}\text{Co}_{25}\text{Ni}_{20}$ HEA under 3.5 wt.% NaCl for 5- and 14-days duration and (b) Electrochemical three electrode flat cell setup.

the weight loss percentage during this period. Also, as per the ASTM-G31-12a [13], Standard Guide for Laboratory Immersion Corrosion Testing of Metals, the average corrosion rates have also been determined by the weight-loss method, which determined from the equation:

$$\text{Corrosion rate}(\text{mm}/\text{year}) = \frac{CW}{ATD} \quad (1)$$

Where, C is constant (8.76×10^4), W is the total weight loss in gram, A is the exposed area of the sample in cm^2 , T is the exposing time in hour, and D is the density of the alloy in g/cm^3 . This method is applicable to uniform corrosion. Non-equiatomically $\text{Cr}_{20}\text{Mn}_{15}\text{Fe}_{20}\text{Co}_{25}\text{Ni}_{20}$ HEA has initial weight of 4.962 gm and density of 8.96 g/cm^3 .

At the immersion test, all the anodic and cathodic reaction rates on electrode surface is zero or the total anodic current is equal to the total cathodic current at the potential (OCP). As the result current will be approximately equal to zero.

Results and Discussion

Immersion test results

The surface after corrosion testing in immersion test for the duration of 5 days and 14 days duration has been observed for non-equiatomically $\text{Cr}_{20}\text{Mn}_{15}\text{Fe}_{20}\text{Co}_{25}\text{Ni}_{20}$ HEA under 3.5 wt.% NaCl solution. The surfaces got corroded severely with a greater number of pits and scratches on the surface. The corrosion obtained on the surface is pitting corrosion as shown in figure 2b for the 5 days duration and figure 2c for the 14 days duration in S1 sample. The intensity of pitting corrosion in sample S1 is less as compared to SS316L. More number of scratches can be seen on sample S1 and number of pits per area is more. Based on the literature survey, addition of more concentration of Mn leads to the detrimental effect on pitting corrosion resistance of stainless steel in 3.5 wt.% NaCl solution [14]. By this we can say that sample with lesser value of Mn composition will have better corrosion resistance as compared to other two samples. With 14 days duration, major changes have been observed in the form of increased size of pits.

Comparison has been made for corrosion rate (mm/year) using weight loss method for non-equiatomically $\text{Cr}_{20}\text{Mn}_{15}\text{Fe}_{20}\text{Co}_{25}\text{Ni}_{20}$ HEA sample in 3.5 wt.% NaCl solution and from table 1, it can be observed that S1 has lower corrosion rate as compared to 304L SS.

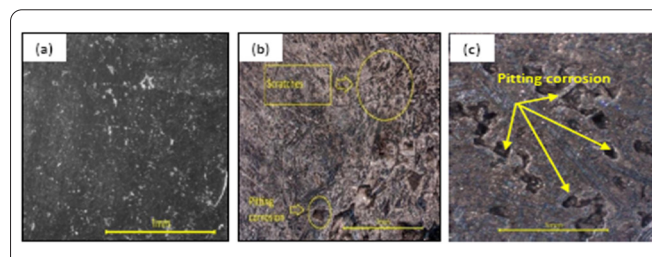


Figure 2: Microscopic images of post immersion testing for the sample in 3.5 wt.% NaCl solution. (a) surface before corrosion, (b) after 5 days duration, and (c) after 14 days duration.

Table 1: Comparison of corrosion rates (mm/year) of HEAs and conventional alloys in the 3.5 wt.% NaCl solution at room temperature.

Sample	Corrosion rate (mm/year) *
S1 (Non-equiatomic)	0.32
304L SS	0.47 [1]
Cu alloy	0.30 [1]

*Average corrosion rates are obtained, including electrochemical measurements and the weight-loss method.

Electrochemical test results

Sample of the non-equiatomic $\text{Cr}_{20}\text{Mn}_{15}\text{Fe}_{20}\text{Co}_{25}\text{Ni}_{20}$ HEA was processed in electrochemical three electrode flat cell setup. The optical microscopic images pre and post corrosion are shown in figure 2. One can easily observe the pitting corrosion spots.

The surface topology and surface roughness profile can be observed from figure 3. Surface has the etched pits due to chemical erosion. S1 sample has $0.571 \mu\text{m}$ roughness before test and $1.879 \mu\text{m}$ after 14 days of immersion test. NaCl solution leads to form chlorides of alloy. Due to the 14 days test, we were able to calculate corrosion rate per year of the sample.

SEM (scanning electron microscope) images of the electrochemical etched sample are shown in figure 4. One can easily observe the inclusions and the pitting on the magnified image after corrosion. Surface get oxidized faster due to anodic and cathodic reactions on the surface on supply of current.

Potentiodynamic polarization results

In this potentiodynamic polarization test, Tafel plot has drawn for NaCl solution under multiple trials to insure the accurate results for analysis with different conventional alloys.

The Tafel plot has been drawn between potential (V vs Ag/AgCl) vs current density (A/cm^2) for the sample under NaCl chemical solution. The increase of corrosion potential and decrease of corrosion current density shows that the corrosion resistance property of the alloy has improved. Metastable pitting (metastable pitting happens due to the initiation and passivation of the pits on the metal surfaces) has also been not observed in the sample. In salt water, the Cl^- anions are detrimental to their nature which destroy the passive layer by penetrating the oxide film at weak points (where the passive films are relatively loose). The common corrosion mode in the Cl^- containing solutions is pitting corrosion. Figure 5 shows that S1 has the E_{corr} value of -319 mV and the I_{corr} value of $-5.099 \text{ A}/\text{cm}^2$. Mn is helping in forming unstable Mn oxides leading to low passive film stability thus it reduces the corrosion resistance of stainless steel (SS). Thus, the S1 has the outstanding corrosion resistance in comparison to other samples of 304 and 201 SS bulk materials at room temperature.

Impedance spectra were used to determine the electrochemical and corrosion behaviour of non-equiatomic Co-CrFeMnNi HEAs in 0.6 M NaCl solution. In this, we have plotted the EIS plots, which are the Nyquist plot and Bode plot. In the Nyquist plots, as shown in figure 5b the measured spectroscopy has shown unfinished semi-circular arcs in all the selected frequency domains. The passive film resistance is directly proportional to the semi-circular arc radius observed in the Nyquist plot. As the semi-circle radius increases, corrosion resistance also increases. From this, we can say that an increase in passive film resistance can be seen from the Nyquist plot for the S1 sample. We can say that alloy with higher Mn composition will experience higher pitting because it is found that Mn has a higher affinity for sulphur and form inclusion (MnS) which in turn starts initiation for pits nucleation.

The Bode-phase angle plot, as shown in figure 6a and 6b also shows that lower depression of phase angle for the S1 sample at the lower frequency region. The higher negative phase angle and broader plateau of phase shift also indicate the superior passive film resistance. The difference in the corrosion resistance is related to the passive films with different elements' composition and integrity formed on the alloy's surfaces.

Conclusions

The corrosion behaviour of non-equiatomic $\text{Cr}_{20}\text{Mn}_{15}\text{Fe}_{20}\text{Co}_{25}\text{Ni}_{20}$ HEA synthesized using low vacuum

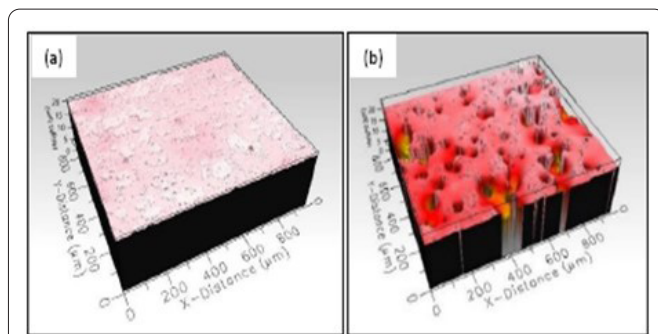


Figure 3: 3D Profilometric images of S1 sample in 3.5 wt.% NaCl solution. (a) Pre-corrosion image and (b) Post corrosion image.

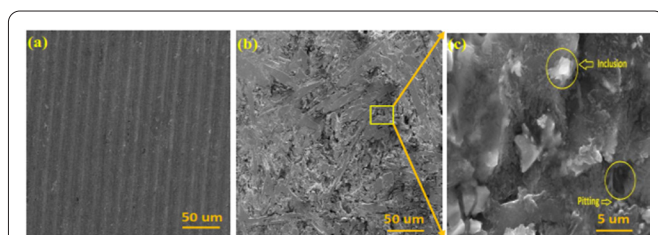


Figure 4: SEM images of non-equiatomic $\text{Cr}_{20}\text{Mn}_{15}\text{Fe}_{20}\text{Co}_{25}\text{Ni}_{20}$ HEA. (a) before corrosion, (b) after electrochemical three electrode flat cell test, and (c) surface at higher magnification.

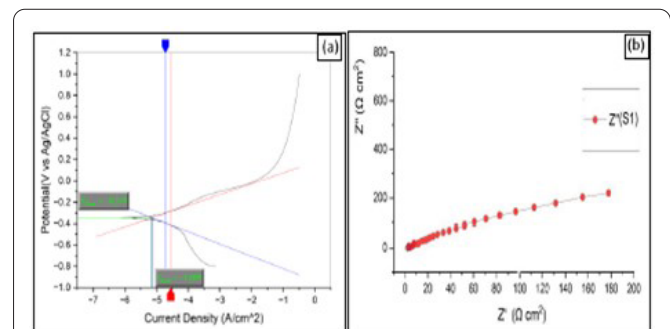
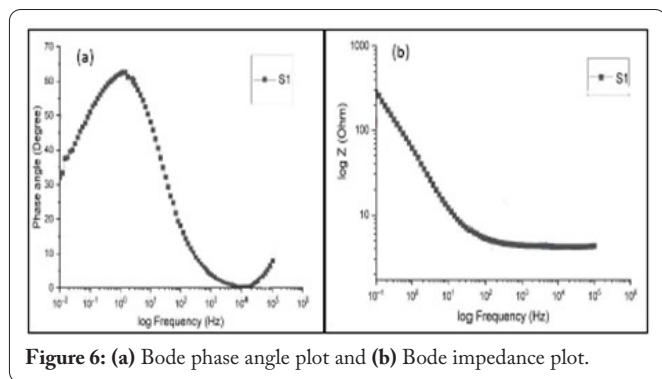


Figure 5: (a) Tafel plot and (b) Nyquist plot for sample S1 in 3.5 wt.% NaCl solution.



induction melting was studied using 3.5 wt.% NaCl solution for immersion test and electrodynamic polarization test. The results were analyzed using stereo-optical microscope, 3D profilometer, SEM and graphs (Tafel plot, Bode impedance plot, and Nyquist plot). Based on the experimental study, the following conclusions can be made:

- The average surface roughness for sample in immersion testing is 1.879 μm at five days and 1.889 μm at 14 days duration.
- In immersion testing, the weight loss percentage obtained for sample for five days and 14 days is 1.02% and 1.44 %, respectively. Corrosion rate obtained using weight loss method is 0.32 mm/year as compared to 0.47 mm/year and 0.30 mm/year for 304L SS and Cu alloy, respectively.
- Tafel plot shows the corrosion potential E_{corr} value of -319 mV and the I_{corr} value of -5.099 A/cm^2 , and highest OCP of -344 mV at 600 seconds, results that sample has increased corrosion resistance capabilities than 304L SS, 201L SS.
- EIS sample has the highest impedance of 945 ohm and lowest frequency of 0.01 Hz and highest negative phase angle of -62.3 degree at lower frequency of 6.81 shows its highest corrosion resistance under NaCl solution against pitting corrosion.
- Post SEM analysis revealed oxides formation, pits, and scratches over the surface. Ni is a less stabilized element among all the other elements. we can say that alloy with higher Mn composition will experience higher pitting because it is found that Mn has a higher affinity for sulphur forming MnS resulting in inclusion forming initiation for pits nucleation.

Acknowledgements

None.

Conflict of Interest

The authors declare that they have no known conflict of interests that could have appeared to influence the work reported in this paper.

Credit Author Statement

Naresh Kaushik: Methodology, Software, Writing - original draft preparation; Anoj Meena: Visualization, Writing - review and editing, Supervision; Vinayak Goswami: Data curation, Validation; Harlal S. Mali: Investigation, Experimentation. All the authors read and approved the manuscript.

References

1. Tang Z, Huang L, He W, Liaw PK. 2014. Alloying and processing effects on the aqueous corrosion behavior of high-entropy alloys. *Entropy* 16(2): 895-911. <https://doi.org/10.3390/e16020895>
2. Yeh JW, Lin SJ. 2018. Breakthrough applications of high-entropy materials. *J Mater Res* 33(19): 3129-3137. <https://doi.org/10.1557/jmr.2018.283>
3. Cantor B, Chang ITH, Knight P, Vincent AJB. 2004. Microstructural development in equiatomic multicomponent alloys. *Mater Sci Eng A* 375: 213-218. <https://doi.org/10.1016/j.msea.2003.10.257>
4. Kaushik N, Meena A, Mali HS. 2022. High entropy alloy synthesis, characterisation, manufacturing & potential applications: a review. *Mater Manuf Process* 37(10): 1085-1109. <https://doi.org/10.1080/10426914.2021.2006223>
5. Praveen S, Murty BS, Kottada RS. 2014. Effect of molybdenum and niobium on the phase formation and hardness of nanocrystalline Co-CrFeNi high entropy alloys. *J Nanosci Nanotechnol* 14(10): 8106-8109. <https://doi.org/10.1166/jnn.2014.9441>
6. Fu Y, Li J, Luo H, Du C, Li X. 2021. Recent advances on environmental corrosion behavior and mechanism of high-entropy alloys. *J Mater Sci Technol* 80: 217-233. <https://doi.org/10.1016/j.jmst.2020.11.044>
7. Qiu X. 2018. Microstructure, hardness and corrosion resistance of $\text{Al}_2\text{CoCrCuFeNiTi}_x$ high-entropy alloy coatings prepared by rapid solidification. *J Alloys Compd* 735: 359-364. <https://doi.org/10.1016/j.jallcom.2017.11.158>
8. Han Z, Ren W, Yang J, Tian A, Du Y, et al. 2020. The corrosion behavior of ultra-fine grained CoNiFeCrMn high-entropy alloys. *J Alloys Compd* 816: 152583. <https://doi.org/10.1016/j.jallcom.2019.152583>
9. Nishimoto A, Fukube T, Maruyama T. 2019. Microstructural, mechanical, and corrosion properties of plasma-nitrided CoCrFeMn-Ni high-entropy alloys. *Surf Coatings Technol* 376: 52-58. <https://doi.org/10.1016/j.surfcoat.2018.06.088>
10. Wang Y, Jin J, Zhang M, Wang X, Gong P, et al. 2021. Effect of the grain size on the corrosion behavior of CoCrFeMnNi HEAs in a 0.5 M H_2SO_4 solution. *J Alloys Compd* 858: 157712. <https://doi.org/10.1016/j.jallcom.2020.157712>
11. Moon JT, Schindelholz EJ, Melia MA, Kustas AB, Chidambaram D. 2020. Corrosion of additively manufactured CoCrFeMnNi high entropy alloy in molten NaNO_3 - KNO_3 . *J Electrochem Soc* 167(8): 081509. <https://doi.org/10.1149/1945-7111/ab8ddf>
12. Kaushik N, Garg H, Meena A, Mali HS. 2021. Materials and design for drogue detection in air-to-air refueling. *Mater Today Proc* 44: 4503-4508. <https://doi.org/10.1016/j.matpr.2020.10.727>
13. ASTM International. Form and Style for ASTM Standards. [https://www.astm.org/media/pdf/bluebook_FormStyle.pdf]
14. Lu CW, Lu YS, Lai ZH, Yen HW, Lee YL. 2020. Comparative corrosion behavior of $\text{Fe}_{50}\text{Mn}_{30}\text{Co}_{10}\text{Cr}_{10}$ dual-phase high-entropy alloy and CoCrFeMnNi high-entropy alloy in 3.5 wt% NaCl solution. *J Alloys Compd* 842: 155824. <https://doi.org/10.1016/j.jallcom.2020.155824>